Single-Channel Properties of Ionic Channels Gated by Cyclic Nucleotides

Giovanna Bucossi,* Mario Nizzari,* and Vincent Torre*#
*INFM, Genova, and #SISSA, Trieste, Italy

ABSTRACT This paper presents an extensive analysis of single-channel properties of cyclic nucleotide gated (CNG) channels, obtained by injecting into *Xenopus laevis* oocytes the mRNA encoding for the α and β subunits from bovine rods. When the α and β subunits of the CNG channel are coexpressed, at least three types of channels with different properties are observed. One type of channel has well-resolved, multiple conductive levels at negative voltages, but not at positive voltages. The other two types of channel are characterized by flickering openings, but are distinguished because they have a low and a high conductance. The α subunit of CNG channels has a well-defined conductance of about 28 pS, but multiple conductive levels are observed in mutant channels E363D and T364M. The conductance of these open states is modulated by protons and the membrane voltage, and has an activation energy around 44 kJ/mol. The relative probability of occupying any of these open states is independent of the cGMP concentration, but depends on extracellular protons. The open probability in the presence of saturating cGMP was 0.78, 0.47, 0.5, and 0.007 in the w.t. and mutants E363D, T364M, and E363G, and its dependence on temperature indicates that the thermodynamics of the transition between the closed and open state is also affected by mutations in the pore region. These results suggest that CNG channels have different conductive levels, leading to the existence of multiple open states in homomeric channels and to the flickering behavior in heteromeric channels, and that the pore is an essential part of the gating of CNG channels.

INTRODUCTION

Cyclic nucleotide gated (CNG) channels from photoreceptors and olfactory sensory neurons form a family of closely related proteins (Kaupp, 1995). CNG channels from vertebrate rods are composed by at least two different subunits, usually referred to as the α (Kaupp et al., 1989) and β subunits (Chen et al., 1993; Körschen et al., 1995). When expressed in *Xenopus laevis* oocytes or cell lines, the α subunit (also referred to here as the w.t.) forms functional channels that are gated by cyclic nucleotides. The ionic selectivity and the shape of the *I-V* relation of the macroscopic current of CNG channels from different species and tissues are broadly similar, although some clear differences in the sensitivity to divalent cations can be observed (Frings et al., 1995). Functional properties of ionic channels formed by the α subunit alone are similar to but not identical to those of the native channel. The β subunit alone does not appear to form functional channels. When the α and β subunits are coexpressed, ionic channels are formed, which are gated by cyclic nucleotides and have properties very similar to those of native channels.

Single-channel properties of CNG channels from different preparations vary in a significant way. The α subunit of the CNG channels from catfish olfactory sensory neurons has three open states with a conductance of about 25, 50, and 80 pS (Goulding et al., 1992; Root and MacKinnon, 1994), and the α subunit of the CNG channel from bovine rods has only one resolvable open state with a conductance of about 28 pS (Kaupp et al., 1989; Nizzari et al., 1993). The α subunit of the CNG channel from bovine olfactory sensory neurons has a single-channel conductance of about 40 pS (Gavazzo et al., 1996). Single-channel openings of the native CNG channel from vertebrate rods are characterized by a very rapid flickering (Sesti et al., 1994), and its mean open time is not longer than 40 μs. Because of this very rapid flickering, the determination of the single-channel conductance is controversial: experiments based on current recordings from patches containing many channels suggested a single-channel conductance of at least 50 pS (Sesti et al., 1994). Recordings from a very limited number of patches containing a single channel indicated a single-channel conductance of 25 pS (Taylor and Baylor, 1995). In contrast, the native CNG channels from bovine olfactory sensory neurons have well-resolved openings with a mean open time larger than 1 ms (Gavazzo et al., 1996).

Recent experimental evidence (Bucossi et al., 1996; Sun et al., 1996) suggests that the pore region is an essential part of the gate and that the closing and opening of the pore are associated with conformational changes within the pore. According to this view, the channel structure has some degree of flexibility, and an analysis of single-channel properties of CNG channels should also be performed in light of this notion.

The aim of this paper is to present an extensive and detailed analysis of single-channel properties of CNG channels and to understand the molecular origin of different single-channel properties found in CNG channels. The collected experimental results on homomeric and heteromeric channels are consistent with the existence of different conducting levels in the CNG channel, leading to the appearance of multiple open states in homomeric channels and to the flickering behavior observed in heteromeric channels.

Received for publication 29 July 1996 and in final form 3 December 1996.
Address reprint requests to Dr. Vincent Torre, SISSA, Via Beirut 2, 34014 Trieste, Italy. Tel.: 39-40-2240470; Fax: 39-40-2240470; E-mail: torre@sissa.it.

0006-3495/97/03/1165/17 $2.00

Mutations in the pore region modify the open probability and the thermodynamics of the transition between the closed and open states, indicating that the channel pore is a major component of the gate of CNG channels and may be directly involved in the allosteric conformational change (Goulding et al., 1994; Gordon and Zagotta, 1995) underlying the transition between the closed and open states.

MATERIALS AND METHODS

Dissection and recording apparatus

Recordings from the α and β subunits of the CNG channel and the mutants (E363D, T364 M, and E363G) were obtained from *Xenopus laevis* oocytes injected with the mRNA encoding for these channels.

Fig. 1 shows the amino acid sequence of the putative pore region of the α and β subunits from CNG channels obtained from different tissues and animals. The sequence alignment indicates a high degree of homology, with some remarkable exceptions (see below).

The mRNA for the α and β subunits (the short version lacking the GARP component; see Körschen et al., 1995) and mutants E363D and E363G was kindly provided by E. Eismann and U. B. Kaupp. The mRNA for mutant T364M was obtained following the procedure described by Sesti et al. (1995). The short version of the β subunit was used because its coexpression with the α subunit leads to the expression of ionic channels with properties very similar to those observed in native photoreceptors (Chen et al., 1993). The mRNA was injected into *X. laevis* oocytes (Centre National de la Recherche Scientifique, Montpellier, France) that were treated as described by Nizzari et al. (1993). Mature *X. laevis* were anesthetized with 0.2% tricainemethanesulphonate (Sigma), and ovarian lobes were removed surgically. The vitelline membrane was removed under visual control in a hyperosmotic medium.

Currents activated by cyclic GMP were recorded under voltage clamp conditions from membrane patches, excised from oocytes, in the inside-out configuration (Hamill et al., 1981). The recording apparatus was the same as that described by Sesti et al. (1995). Approximately 50 nM mRNA was injected into each oocyte, and membrane patches containing a single channel could be obtained after about 18 h of incubation. When the incubation time was longer than 36 h, single-channel recordings were very rare.

Alpha Subunit

Bovrod	348	V Y S L Y W S T L T L T T I G E T P P P V
Bovtestis	373	I Y S L Y W S T L T L T T I G E T P P P V
Drodsrod	300	I Y S F Y W S T L T L T T I G E T P T P E
Chickrod	302	V Y S L Y W S T L T L T T I G E T P P P V
Humanrod	346	V Y S L Y W S T L T L T T I G E T P P P V
Chickcone	395	I Y S L Y W S T L T L T T I G E T P P P V
Ratrod	341	V Y S L Y W S T L T L T T I G E T P P P V
Bovolf	325	I Y C L Y W S T L T L T T I G E T P P P V
Catfisholf	318	V Y C F Y W S T L T L T T I G E [M] P P P V
Ratolf	327	I Y C L Y W S T L I L T T I G E T P P P V

Beta Subunit

Rodbov	947	I R C Y Y W A V K T L I T I G [G] L P D P R
Ratolf	329	L Y S F Y F S T L I L T T V G [D] T P L P D

FIGURE 1 The amino acid sequence in the putative pore region of the α subunit of cyclic nucleotide gated channels from bovine rods (Kaupp et al., 1989), bovine testis (Weyand et al., 1994), drosophila photoreceptors (Baumann et al., 1994), chick rods (Bönigk et al., 1993), human rods (Dhallan et al., 1992), chick cones (Bönigk et al., 1993), mouse rods (Baehr et al., 1992), bovine olfactory sensory neurons (Ludwig et al., 1990), catfish olfactory sensory neurons (Goulding et al., 1992), rat olfactory sensory neurons (Dhallan et al., 1990), and the β subunit from bovine (Körschen et al., 1995) and rat rods (Bradley et al., 1994).

Solutions

The solution filling the patch pipette was composed of 110 mM NaCl, 2 mM EDTA, and 10 mM HEPES buffered to pH 7.6 with tetramethylammonium hydroxide (TMAOH) or NaOH. Neutralizing the solution with TMAOH or NaOH did not significantly affect either the macroscopic current or the single-channel current. Solutions with a pH of 5.5, 6.0, 6.8, 8.4, and 9.1 were obtained by using 10 mM 2-(*N*-morpholino)ethanesulfonic acid for pH 5.5 and 6.0, 10 mM 2-[(2-amino-2-oxoethyl)-amino]ethanesulfonic acid for pH 6.8, 10 mM *N*-tris[hydroxymethyl]methyl-3-aminopropanesulfonic acid for pH 8.4 and 9.1, and appropriate amounts of NaOH or TMAOH. The procedure for changing the temperature was similar to that described by Sesti et al. (1996).

Determination of single-channel conductances

Several single-channel properties were obtained from the analysis of amplitude histograms of current openings induced by cGMP in membrane patches containing a single CNG channel. A patch was assumed to contain a single CNG channel when channel openings at low cGMP concentrations, i.e. 20 and 35 μM, had amplitudes similar to those observed in the presence of saturating cGMP concentrations, i.e. at 500 and 1000 μM. Figs. 2–4 and 7 show examples of single-channel patches. The single-channel current was determined by analysis of amplitude histograms, normalized so as to have an area of 1. Amplitude histograms were fitted as the sum of two or more Gaussian functions. For instance, the amplitude histogram of mutant T364 M at negative voltages was fitted as

$$a_0 e^{-x^2/2\sigma_0^2} + a_1 e^{-(x-c_1)^2/2\sigma_1^2} + a_2 e^{-(x-c_2)^2/2\sigma_2^2} + a_3 e^{-(x-c_3)^2/2\sigma_3^2}, \quad (1)$$

where c_i is the mean current flowing through the open state o_i, σ_i is the variance of the Gaussian function, and a_i is a suitable normalizing coefficient. In the case of mutant E363D, a_3 was taken to be 0; for the w.t. a_2 was also taken to be 0. The total open probability p_o was assumed to be $1 - p_c$, where p_c was taken to be $a_0\sigma_0\sqrt{2\pi}$, and the open probability p_i, corresponding to the opening to the current level c_i, was taken to be $a_i\sigma_i\sqrt{\pi}$.

Power spectra computation

Power spectra of current fluctuations induced by cGMP were computed as described by Sesti et al. (1994). Data were filtered with an 8-pole Butterworth filter, nominally set at 20 kHz, corresponding to an effective cutoff frequency (50% reduction) of about 10 kHz.

Determination of the activation energy of the single-channel current through an open state

The activation energy of ionic permeation through an open state was estimated by analyzing the relation between the single-channel current and

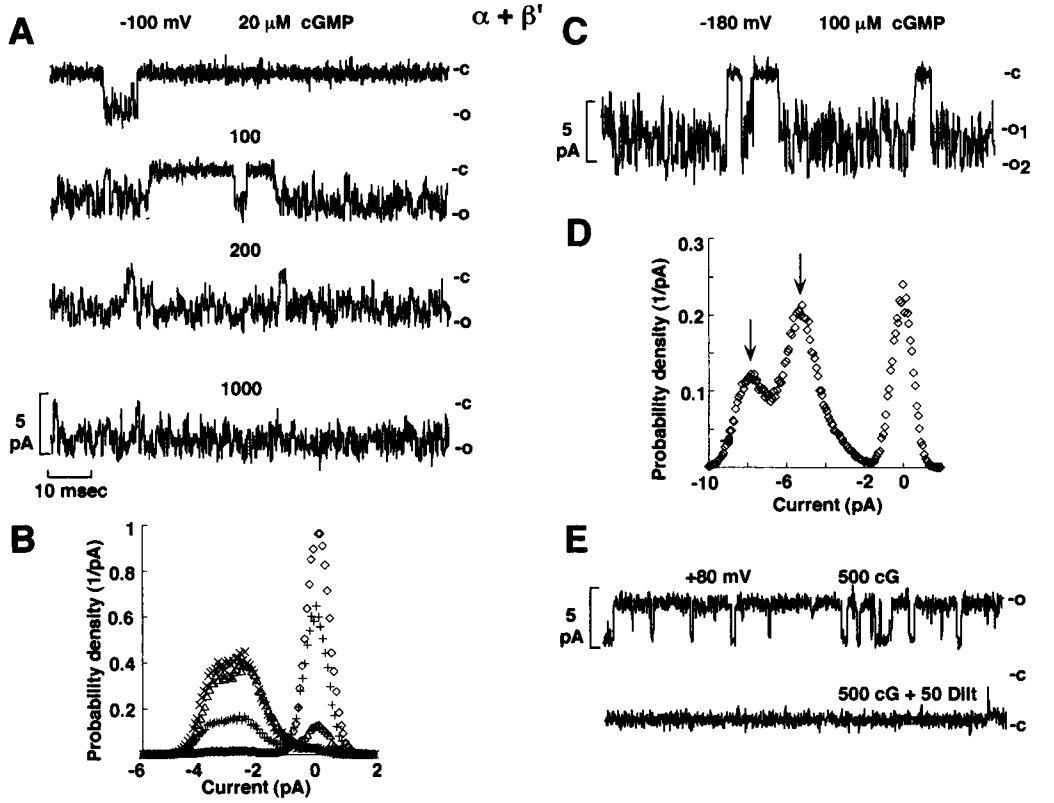

FIGURE 2 Single-channel properties of the coexpression of the α and β subunit: type 1 channel. (*A*) Current recordings at −100 mV in the presence of different amounts of cGMP. (*B*) Amplitude histograms from the experiment illustrated in *A*, in the presence of 20 (◇), 100 (+), 200 (△), and 1000 (×) μM cGMP. (*C*) Current recordings from the same patch as in *A*, but at −180 mV. (*D*) Amplitude histogram of current openings illustrated in *C*. (*E*) Current recordings from the same patch as in *A*, at +80 mV in the presence of 500 μM cGMP (*upper trace*) and in the presence of 50 μM L-*cis*-diltiazem as well (*lower trace*). Current recordings were filtered at 4 kHz and sampled at 20 kHz.

$1/RT$, where R is the gas constant and T is the absolute temperature. The data were plotted on a semilogarithmic scale, and the straight line through the experimental points between 13° and 23° was obtained with a least-mean-square procedure. The slope of this straight line was taken as an estimate of the activation energy, so that the best fit with the equation (see Atkins, 1978),

$$\text{const } e^{-A_c/RT}, \tag{2}$$

provided an estimate of the activation energy A_c of ionic permeation through that open state.

Determination of the Gibbs free energy ΔG_{open} of channel opening

In the presence of a saturating cGMP concentration, the CNG channel is assumed to be in a fully liganded state and the open and the fully liganded closed states are assumed to be in thermodynamic equilibrium. Therefore the Gibbs free energy ΔG_{open} associated with the transition from the closed to the open state of a channel (equivalent to the free energy change of the allosteric transition in Varnum et al., 1995) can be determined from the relation

$$\Delta G_{open} = G_o - G_c = RT \ln \frac{p_c}{p_o}, \tag{3}$$

where $p_o = 1 - p_c$, and p_c is the closed probability in the presence of a saturating cGMP concentration (i.e., 1000 μM). ΔG_{open} characterizes the free energy associated with the channel gating and may be referred to as the gating free energy. The open probability was determined from at least 10 s of continuous recordings, which did not contain long closed states, which can be observed at positive voltages (see Figs. 3, 4, and 10). The open probability computed over at least 10 s of recordings was similar, within 10%, to that obtained from shorter recordings of about 2 s. The gating free energy ΔG_{open} is equal to $\Delta H_{open} - T\Delta S_{open}$, where ΔH_{open} is the enthalpic contribution and $T\Delta S_{open}$ is the entropic contribution. ΔS_{open} was determined as

$$\Delta S_{open} = -\frac{\Delta G_{open}}{dT}. \tag{4}$$

ΔS_{open} was obtained from a linear best fit of the relation between ΔG_{open} and temperature (see Fig. 13) in the range between 8° and 23°.

RESULTS

When the mRNA of the α subunit is injected into *X. laevis* oocytes, CNG channels with well-resolved openings can be observed (Kaupp et al., 1989; Nizzari et al., 1993). However, native CNG channels from vertebrate rods are characterized by very brief and flickering openings originated by the additional presence of the β subunit (Chen et al., 1993). Therefore we have analyzed single CNG channels obtained by the coexpression of the α and β subunits in oocytes.

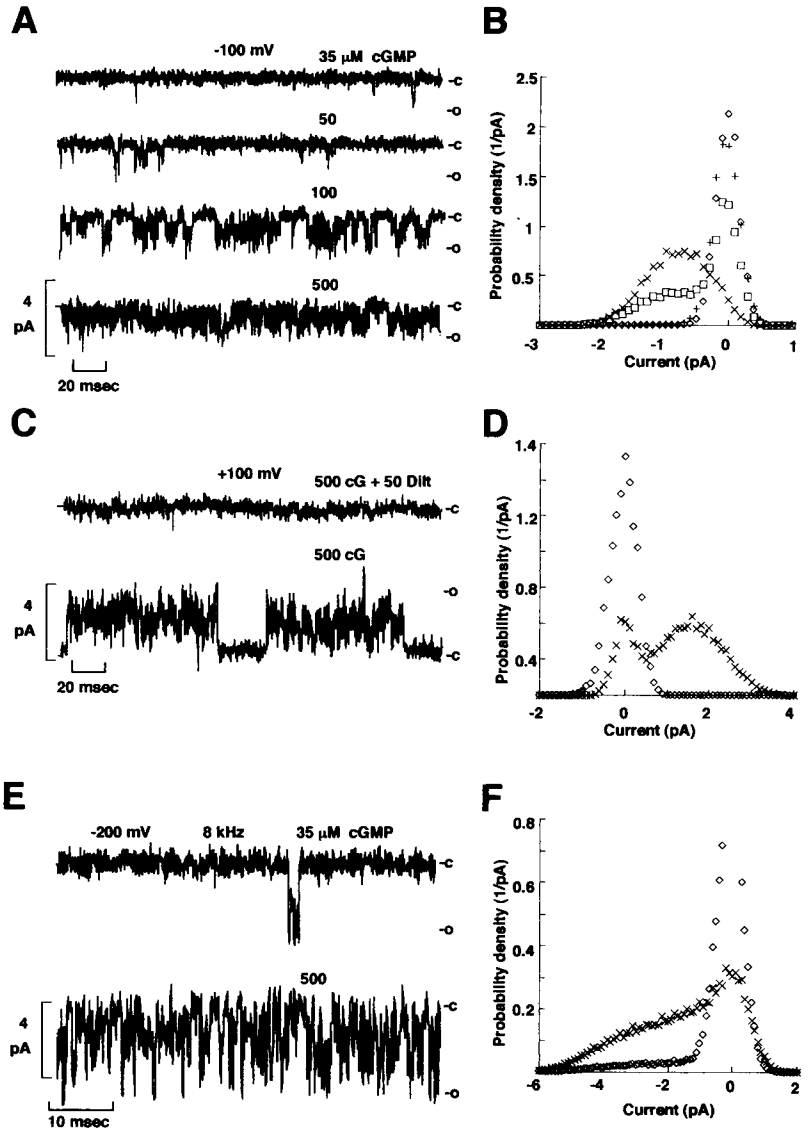

FIGURE 3 Single-channel properties of the coexpression of the α and β subunit: type 2 channel (low conductance). (*A*) Current recordings at -100 mV in the presence of different concentrations of cGMP. (*B*) Amplitude histograms from the experiment illustrated in *A*, in the presence of 35 ($\diamond$), 50 (+), 100 ($\square$), and 500 ($\times$) μM cGMP. (*C*) Current recordings from the same patch as in *A* at $+100$ mV in the presence of 500 μM cGMP (*lower trace*) and in the presence of 50 μM L-*cis*-diltiazem as well (*upper trace*). (*D*) Amplitude histograms of current recordings shown in *C*, in the absence ($\times$) and in the presence ($\diamond$) of diltiazem. Current recordings in *A* and *C* filtered at 4 kHz and sampled at 20 kHz. (*E*) Current recordings from the same patch as in *A* and *C*, but at -200 mV, filtered at 8 kHz and sampled at 40 kHz. (*F*) Amplitude histograms of current recordings shown in *E*. Symbols as in *B*.

The coexpression of the α and β subunits

The analysis of patches containing a single CNG channel, obtained by coinjecting the mRNA for the α and β subunits (in the ratio 1/2.5), indicated the existence of different types of channel. To distinguish recordings from a patch containing a single CNG channel from recordings from several CNG channels, the following criterion was adopted: a patch was considered to contain a single CNG channel when current transients observed at low and high cGMP concentrations had a similar amplitude (see Figs. 2–4). Among more than 50 recordings from presumed single-channel patches, 29 satisfied this criterion. In four of these channel recordings, a single well-resolved opening was observed at positive voltages, but multiple openings were detected at negative voltages. These channels were classified as type 1 channels (see Fig. 2). The remaining 25 patches exhibited highly flickering openings, very similar to those described in the native channel (Sesti et al., 1994; Taylor and Baylor, 1995) and in previous reports (Chen et al., 1993; Körschen et al., 1995). However, these 25 patches exhibited channel openings of different amplitude varying by more than 100%, which was most remarkable at $+100$ mV, and were classified as type 2 and 3 channels. Type 2 channels had a low conductance (see Fig. 3), and type 3 channels had a high conductance (see Fig. 4).

Fig. 2 illustrates current recordings from type 1 channel obtained by coexpressing the α and β subunits. Fig. 2 *A* reproduces current recordings at -100 mV in the presence of different cGMP concentrations (20, 100, 200, and 1000 μM); the corresponding amplitude histograms are shown in Fig. 2 *B*. These openings were noisier than those observed in the w.t. channel (compare with Fig. 6), but the amplitude histogram showed a broad, well-resolved peak corresponding to the open state at all cGMP concentrations (see Fig. 2 *B*). When current transients were observed at -180 mV (see Fig. 2 *C*), the amplitude histogram corresponding to channel

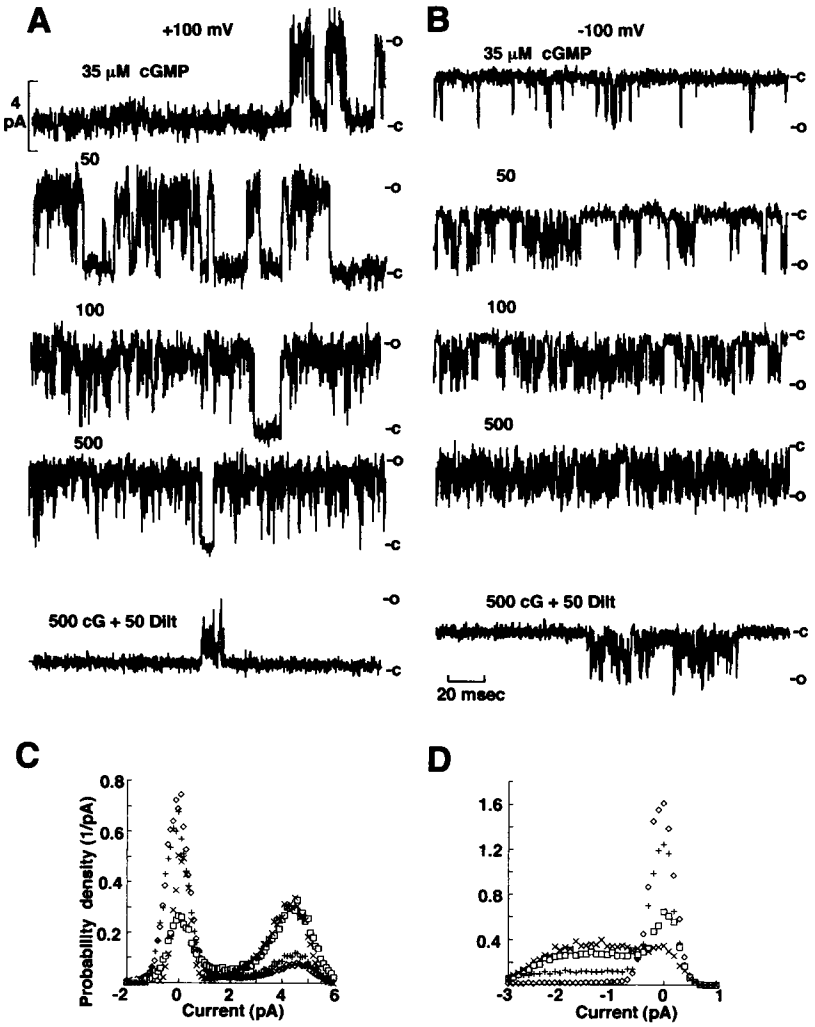

FIGURE 4 Single-channel properties of the coexpression of the α and β subunit: type 3 channel (high conductance). (*A* and *B*) Current recordings at +100 (*A*) and at −100 mV (*B*) in the presence of different concentrations of cGMP and in the presence of 500 μM cGMP and 50 μM L-*cis*-diltiazem (*lower traces*). (*C* and *D*) Amplitude histograms of current opening from the experiment illustrated in *A* and *B*, respectively, in the presence of 35 (◇), 50 (+), 100 (□), and 500 (×) μM cGMP. Current recordings were filtered at 4 kHz and sampled at 20 kHz.

openings (see Fig. 2 *D*) revealed two well-resolved peaks corresponding to conductances of about 30 and 44 pS, respectively. A less resolved conductance level of about 15 pS can be noticed by visual inspection of current recordings of Fig. 2 *C*. Homomeric CNG channels are not significantly blocked by the compound L-*cis*-diltiazem (Kaupp et al., 1989), whereas native CNG channels from photoreceptors are (Stern et al., 1986). Therefore the effect of L-*cis*-diltiazem on heteromeric channels was investigated (see also Chen et al., 1993; Körschen et al., 1995). At +80 mV, the type 1 channel had well-resolved openings, which were completely blocked by the addition of 50 μM L-*cis*-diltiazem (see Fig. 2 *E*). The single-channel conductance at +80 mV was approximately 40 pS. When the membrane voltage was returned to −100 mV, a single current level was observed and no changes in single-channel properties were observed over time.

Type 2 and 3 channels have highly flickering openings at both positive and negative voltages (see Figs. 3 and 4). Fig. 3 *A* reproduces current recordings at −100 mV from type 2 channel in the presence of different cGMP concentrations (35, 50, 100, and 500 μM); the corresponding amplitude histograms are shown in Fig. 3 *B*. Fig. 3 *C* shows current recordings in the presence of 500 μM cGMP at +100 mV in the absence (*lower trace*) and in the presence (*upper trace*) of 50 μM L-*cis*-diltiazem, indicating that the channel openings were almost completely blocked by L-*cis*-diltiazem. The corresponding amplitude histograms are shown in Fig. 3 *D*.

At positive voltages, current openings were often interrupted by long closed times, even in the presence of saturating cGMP concentrations. At +100 mV the amplitude histogram revealed a well-resolved peak corresponding to the open state, whereas at −100 mV it did not show two distinct peaks corresponding to the open and closed states. This behavior is almost identical to that described by Taylor and Baylor (1995) in some recordings from single-channel patches excised from rod outer segments.

To resolve channel openings it may be useful to apply larger voltages and record the electrical activity at a wider bandwidth. Fig. 3 *E* illustrates current recordings from the same patch as in Fig. 3 *A*, but at −200 mV and at a bandwidth of 8 kHz. Amplitude histograms are shown in Fig. 3 *F*. Even in the presence of a larger driving force, no

square events could be detected and amplitude histograms were simply broader.

Fig. 4 illustrates current recordings from a type 3 channel. Fig. 4, *A* and *B*, reproduces current recordings at +100 and − 100 mV, respectively, in the presence of different cGMP concentrations; the corresponding amplitude histograms are shown in Fig. 4, *C* and *D*, respectively. Channel openings have the same amplitude at low and high cGMP concentrations, and the shape of the amplitude histogram corresponding to openings does not change while increasing the cGMP level. These observations indicate that the recording was from a patch containing a single CNG channel. The analysis of amplitude histograms at +100 mV indicates that this channel has a single-channel conductance of at least 45 pS. The lower traces in Fig. 4, *A* and *B*, were obtained in the presence of 500 μM cGMP and 50 μM L-*cis*-diltiazem, at +100 and −100 mV, respectively. It is evident that this channel was blocked by L-*cis*-diltiazem in a voltage-dependent way. Type 3 channel appeared to be slightly more sensitive to cGMP and L-*cis*-diltiazem than type 1 or 2. However, the sensitivity of these channels to cGMP and L-*cis*-diltiazem was not investigated in detail. The kinetics of heteromeric channels, especially types 2 and 3, was too fast to measure open and closed states; as a consequence, we have not attempted to measure these quantities.

Fig. 5 illustrates the distribution of the apparent conductance of flickering channels at −100 (*broken line*) and +100 mV (*solid line*). The apparent conductance was obtained as I_{peak}/V. At −100 mV, I_{peak} was the current corresponding to the peak of the amplitude histogram in the presence of 500 or 1000 μM cGMP; at +100 mV I_{peak} was the current of the peak of the amplitude histogram corresponding to the open state. At −100 mV the distribution had a single peak between 5 and 10 pS. At +100 mV the distribution of the apparent conductance indicated the existence of channels with a low conductance (type 2) and channels with a high conductance (type 3).

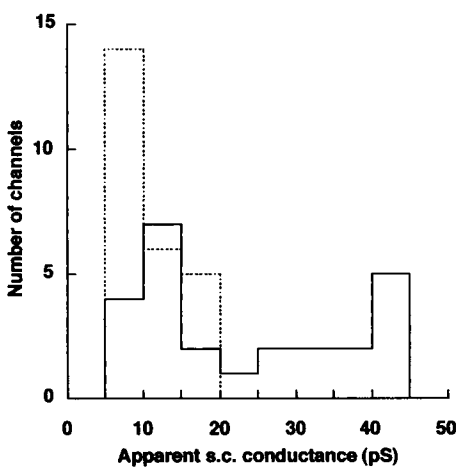

FIGURE 5 Distribution of apparent conductance of single channels at −100 (– – –) and at +100 mV (——). The apparent conductance at −100 mV was obtained as I_{peak}/V. At −100 mV, I_{peak} was the current corresponding to the peak of the amplitude histogram in the presence of 1000μM cGMP; at +100 mV I_{peak} is the current of the peak of the amplitude histogram corresponding to the open state. Data from 25 single-channel recordings.

Assuming that at +100 mV type 2 channels have an apparent conductance between 5 and 25 pS and type 3 channels between 25 and 45 pS, the fraction of flickering channels of types 2 and 3 was 0.56 and 0.44, respectively.

The analysis of similarities and differences in the amino acid sequence of the α and β subunits in the putative pore region (see Fig. 1) can provide useful information for the understanding of the molecular mechanisms underlying the flickering behavior of heteromeric CNG channels. At the equivalent location 363 of the bovine rods, all α subunits have a glutamate that controls features of ionic permeation such as rectification, blockage by extracellular divalent cations, and the multi-ion nature of the channel (Root and MacKinnon, 1993; Eismann et al., 1994; Park and MacKinnon, 1995; Sesti et al., 1995). At the equivalent position 364 of the bovine rod, all CNG channels have a threonine, with the exception of the CNG channel from catfish olfactory sensory neurons, which has a methionine. Therefore we have studied the properties of mutant T364M (18 single-channel patches) of the α subunit of CNG bovine rods. The putative pore region of the β subunit of CNG channels has a lower homology with the family of the α subunits. However, it is important to notice that at location 363 of the CNG channel from bovine rods, where a critical glutamate is located, the β subunit from bovine rods has a glycine, whereas the β subunit from rat olfactory neurons has an aspartate. The so-called β subunit from olfactory sensory neurons, however, may be another α subunit and not a distinct phylogenetic protein (Kaupp, 1995). Because of the critical role of glutamate 363 in the α subunit, we have investigated in detail the properties of mutants E363G (eight patches and three single-channel patches) and E363D (20 single-channel patches) of the α subunit of CNG channel from bovine rods.

Mutants E363D and T364M

Fig. 6 illustrates current recordings from membrane patches containing a single channel gated by cGMP of the w.t. and of mutants E363D and T364M at −100 mV (*A*) and +100 mV (*B*). The channels were activated by the addition of 500 μM cGMP to the medium bathing the intracellular side of the membrane. Analysis of current recordings and of amplitude histograms indicates that the w.t. channel has a well-resolved conductance of about 28 pS at both positive and negative membrane voltages. The sum of two Gaussian functions, however, does not provide a good fit of the amplitude histogram, possibly suggesting the existence of substates that could not be well resolved. At −100 mV, however, mutant E363D exhibits noisier openings, and the analysis of amplitude histograms indicates the existence of at least two open states with conductances of about 28 and 46 pS (see *arrows* in the middle amplitude histogram in Fig.

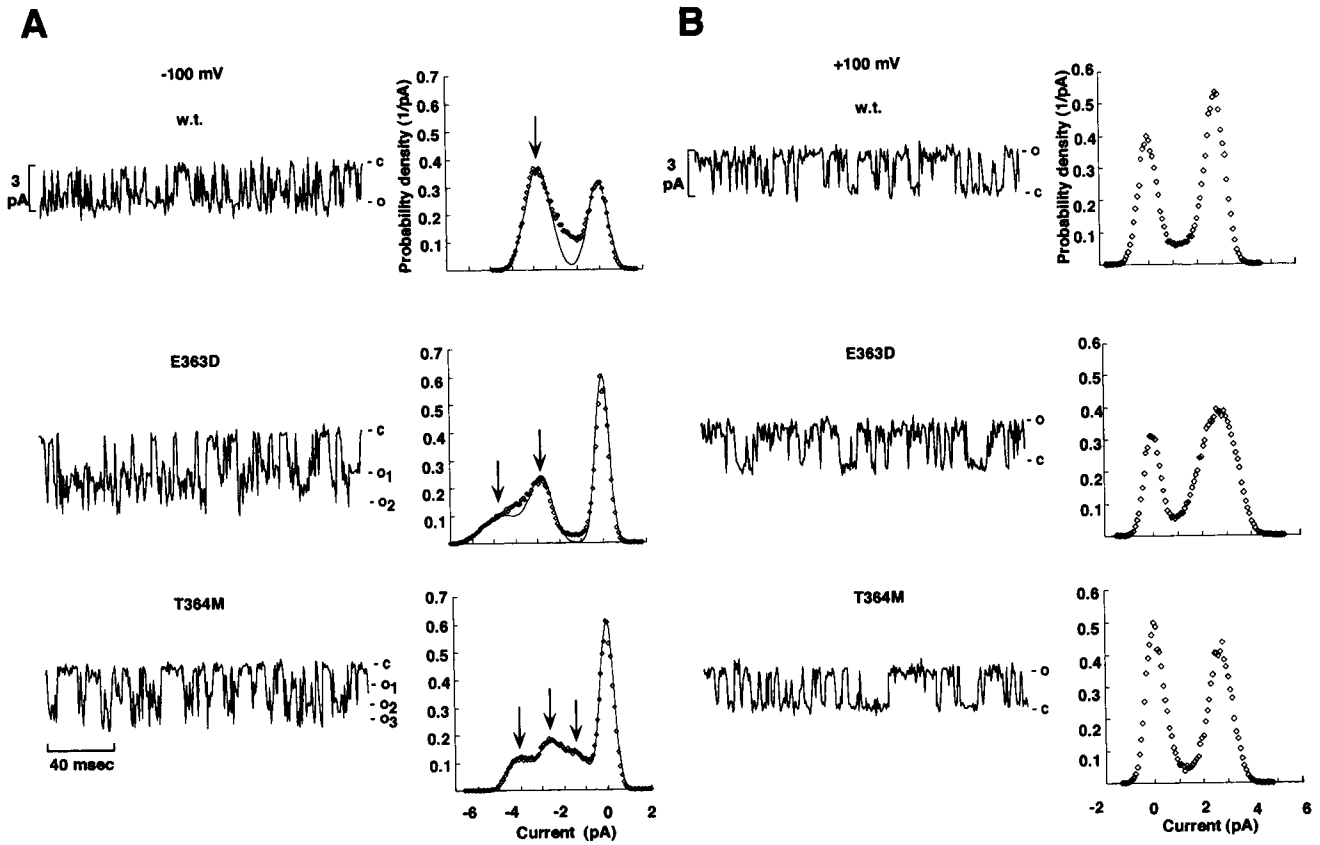

FIGURE 6 The single-channel current of the w.t. and mutants E363D and T364M at −100 (*A*) and +100 mV (*B*). Channels were activated by 500 μM cGMP added to the medium bathing the intracellular side of the membrane. Current recordings were filtered at 4 kHz and sampled at 20 kHz. Amplitude histograms were obtained from at least 8 s of current recordings. Upper, middle, and lower rows refer to the w.t. and mutants E363D and T364M, respectively. Amplitude histograms at −100 mV were fitted as the sum of two (for the w.t.), three (for mutant E363D), and four (for mutant T364M) Gaussian functions. The parameter values used to obtain the fitting were $a_0 = 0.32$, $\sigma_0 = 0.44$ pA, $a_1 = 0.37$, $\sigma_1 = 0.57$ pA, and $c_1 = -2.8$ pA for the w.t.; $a_0 = 0.6$, $\sigma_0 = 0.31$ pA, $a_1 = 0.18$, $\sigma_1 = 0.54$ pA, $c_1 = -2.8$ pA, $a_2 = 0.12$, $\sigma_2 = 0.63$ pA, and $c_2 = -4.6$ pA for mutant E363D; $a_0 = 0.1$, $\sigma_0 = 0.33$ pA, $a_1 = 0.125$, $\sigma_1 = 0.54$ pA, $c_1 = -1.7$ pA, $a_2 = 0.155$, $\sigma_2 = 0.5$ pA, $c_2 = -2.6$ pA, $a_3 = 0.120$, $\sigma_3 = 0.63$ pA, and $c_3 = -4.3$ pA for mutant T364M.

6 *A*). At the same voltage, mutant T364M has three distinct open levels with conductances of about 17, 25, and 43 pS (see *arrows* in the lower amplitude histogram in Fig. 6 *A*). The distinct open state levels observed in mutant T364M are very similar to those already described in the CNG channel from catfish olfactory sensory neurons (Goulding et al., 1992; Root and MacKinnon, 1994).

At +100 mV, amplitude histograms of current fluctuations of the w.t. and mutant T364M have only two peaks with a similar and symmetrical shape, indicating the existence of only one resolvable conductance level. The same conclusion was reached during the analysis of a patch containing a single CNG channel of mutant T364M, in which it was possible to study channel openings up to +200 mV. In mutant E363D, at +100 mV, the lobe of the amplitude histogram corresponding to the open state is significantly broader than that corresponding to the closed state, suggesting the existence of distinct open states with a single-channel conductance of about 30 pS. Similarly, single-channel current recordings from w.t. channels at −200 mV were significantly noisier during the open state than the closed state: the standard deviation of the open state was four times that of the closed state. These results suggest that the w.t. channel also has distinct open states with a similar conductance around 30 pS. Single-channel properties of the w.t. and mutant channels E363D and T364M were remarkably consistent in all single-channel patches, and the single-channel conductance did not vary by more than 10%.

The amplitude histograms shown in Fig. 6 were obtained in the presence of a high concentration of cGMP (i.e., 500 μM); therefore we have examined the possibility that the occurrence of the different conducting open states of mutants E363D and T364M depends on the cGMP concentration.

Fig. 7, *A* and *B*, reproduces current recordings obtained in the presence of different cGMP concentrations from membrane patches containing a single channel of mutants E363D and T364M, respectively. Amplitude histograms of current fluctuations in the presence of different cGMP concentrations are shown in Fig. 7, *C* and *D*, for mutants E363D and T364M, respectively. Amplitude histograms associated with channel openings (i.e., between −6 and −1 pA) can be fitted by the same equation, properly scaled, as shown by

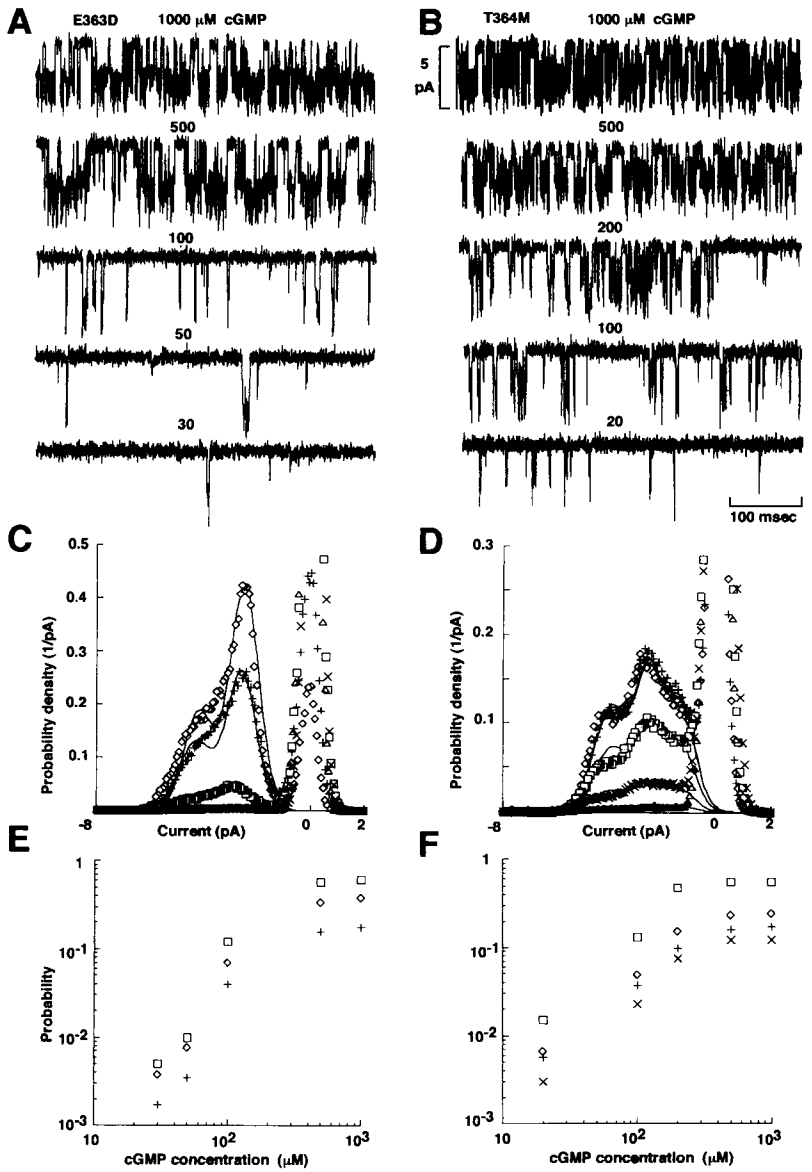

FIGURE 7 The dependence of open substates of mutants E363D and T364M on the cGMP concentration. (*A* and *B*) Current recordings at −100 mV obtained in the presence of the indicated cGMP concentration from a membrane patch containing a single channel activated by cGMP of mutants E363D and T364M, respectively. (*C* and *D*) Amplitude histograms in the presence of different levels of cGMP. (*C*) 30 (△), 50 (×), 100 (□), 500 (+), and 1000 (◇) μM cGMP; (*D*) 20 (△), 100 (×), 200 (□), 500 (+), and 1000 (◇) μM cGMP. The continuous lines in *C* were obtained as the sum of two Gaussian functions with $a_1 = 0.18$, $\sigma_1 = 0.54$ pA, $c_1 = -2.8$ pA, $a_2 = 0.12$, $\sigma_2 = 0.63$ pA, and $c_2 = -4.6$ pA, appropriately scaled. The continuous lines in *D* were obtained as the sum of three Gaussian functions with $a_1 = 0.125$, $\sigma_1 = 0.54$ pA, $c_1 = -1.7$ pA, $a_2 = 0.155$, $\sigma_2 = 0.5$ pA, $c_2 = -2.6$ pA, $a_3 = 0.12$, $\sigma_3 = 0.63$ pA, and $c_3 = -4.3$ pA, appropriately scaled. (*E* and *F*) Relation between cGMP concentration and open probability: p_o (□), p_1 (◇), and p_2 (+) for mutant E363D in *E* and p_o (□), p_1 (◇), p_2 (+), and p_3 (×) for mutant T364 M in *F*. Open probabilities were determined as described in Materials and Methods.

the theoretical lines through the experimental points in Fig. 7, *C* and *D*. Fig. 7, *E* and *F*, shows the dependence of the total open probability p_o and of the open substates p_i on the cGMP concentration for mutants E363D and T364M, respectively. It is evident that the relative probability of the different open states does not depend on the level of channel agonist. These results were observed in three single-channel patches of mutants E363D and T364M.

Mutant E363G

As shown in Fig. 1, the β subunit from bovine rods has a glycine at the equivalent position of glutamate 363 of the rod channel. As the amino acid in position 363 controls several features of ionic permeation (Root and MacKinnon, 1993; Eismann et al., 1994; Park and MacKinnon, 1995; Sesti et al., 1995), the fast flickering of the native channel may be caused by the presence of a glycine in the β subunit; therefore we have investigated the mutant E363G.

Fig. 8 *A* illustrates current recordings at −100 mV, in the presence of different levels of cGMP (0, 100, 200, 500, and 1000 μM), from a patch containing several channels of mutant E363G. The mean current in the presence of 500 and 1000 μM cGMP was 1.75 and 1.9 pA, respectively, indicating that 1000 μM cGMP activated mutant E363G almost completely. At 22°C these openings are very brief and transient. In a previous study (Sesti et al., 1996) it was shown that when the temperature is decreased, square events can be detected, and the single-channel conductance at 18°C is about 30 pS.

Fig. 8 *B* illustrates current recordings at −140 mV from a membrane patch presumably containing a single CNG channel of mutant E363G. In the absence of cGMP the trace is quiet (Fig. 8 *B*, *upper trace*), and upon addition of 1000

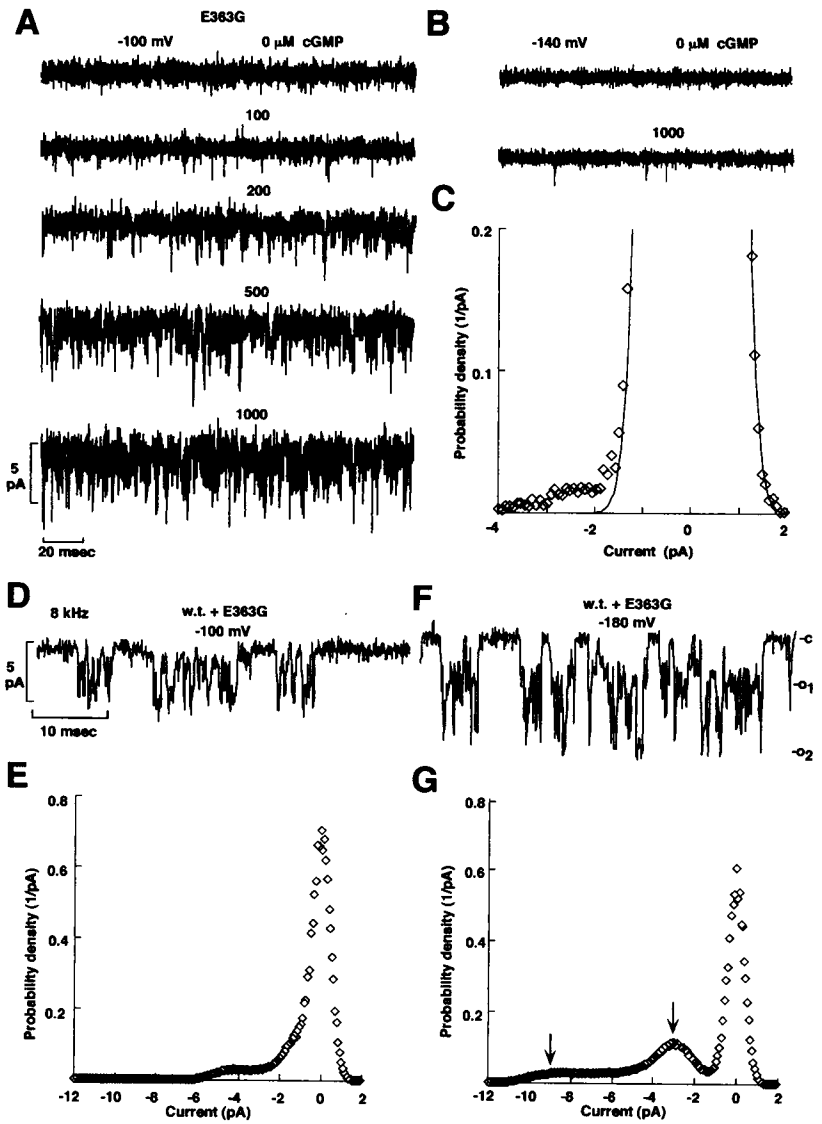

FIGURE 8 Single-channel properties of mutant E363G. (*A*) Current recordings at −100 mV from a membrane patch containing several mutant channels E363G activated by cGMP in the presence of different concentrations of cGMP. (*B*) Current recordings from a patch presumably containing a single mutant channel E363G. The upper and lower traces were obtained in the absence of cGMP and in the presence of 1000 μM cGMP, respectively, at the holding voltage of −140 mV. Current recordings in *A* and *B* had the same scales and were filtered at 4 kHz and sampled at 20 kHz. (*C*) Amplitude histogram from 25 s of the current recording shown in *B* in the presence of cGMP. (*D–G*) Single-channel properties of the coexpression of the w.t. and mutant E363G. The mRNA of the w.t. and mutant E363G were coinjected in the ratio of 1:2 in oocytes. (*D* and *F*) Current recordings in the presence of 500 μM cGMP at −100 and −180 mV, respectively. (*E* and *G*) Amplitude histograms obtained at the holding voltage of −100 and −180 mV, respectively.

μM cGMP, brief and rare openings are observed (Fig. 8 *B*, *lower trace*). In agreement with previous reports (Sesti et al., 1996), when the temperature was decreased to about 10°C, well-resolved openings were observed in the presence of cGMP, but not in its absence. Fig. 8 *C* reproduces the amplitude histogram of current fluctuations from the experiment shown in Fig. 8 *B*, where the solid line is a Gaussian distribution corresponding to the noise of the closed state. By computing the area of the histogram above the Gaussian distribution and corresponding to channel openings, the open probability was estimated to be on the order of 0.007 (see also Sesti et al., 1996). Under similar conditions, the open probability of the w.t. is around 0.8, i.e., almost 100-fold that of mutant E363G. As a consequence, a mutation in the pore region profoundly modifies the gating of CNG channels.

Fig. 8 *D* reproduces current recordings from a CNG channel obtained by coinjecting the mRNA for the w.t. and mutant E363G into oocytes in the ratio 1/2. In the presence of 500 μM cGMP and at −100 mV (Fig. 8 *D*), channel openings were rather transient and reminiscent of those observed in the native channel. The amplitude histogram (see Fig. 8 *E*) did not show a clear second peak corresponding to a well-resolved opening. However, when current fluctuations were studied at −180 mV (see Fig. 8 *F*), the amplitude histogram (see Fig. 8 *G*) exhibited a well-resolved peak corresponding to a conductance of about 17 pS and a tail corresponding to much larger openings with conductances up to about 50 pS. Because of the significant flickering, the number of the conductance levels above that at 17 pS could not be determined. The behavior described in Fig. 8, *F* and *G*, was also observed in another four single-channel recordings, but the lowest conductance level varied between 15 and 25 pS, and the highest one ranged between 40 and 60 pS. The openings of mutant E363G are reminiscent of those observed in heteromeric type 1 channel (see Fig. 2). It is worth noticing that both the w.t. and mutant E363G have a single-channel conductance of about 30 pS,

but when they are heterologously coexpressed, heteromeric channels have at least two open states with conductances above and below 30 pS.

The effect of external and internal pH

The relative probability of the different open states of the CNG channels from catfish olfactory sensory neurons depends on pH (Goulding et al., 1992; Root and MacKinnon, 1994). Therefore, to understand the physical properties of the different open states observed in CNG channels from vertebrate rods, we have analyzed the effect of extracellular and intracellular pH on the different open states of mutants E363D and T364M and on channels obtained from the coexpression of the α and β subunits.

Fig. 9 illustrates the effect of changing the extracellular pH on channel openings induced by 500 μM cGMP in mutants E363D (Fig. 9 *A*) and T364M (Fig. 9 *B*), at -140 mV. Current recordings in Fig. 9, *A* and *B*, were obtained from different patches because the solution filling the patch pipette could not be changed during an experiment. When the proton concentration in the extracellular medium was reduced (i.e., $[pH]_o$ was increased to 8.4), openings of mutant T364M were more squared and, to a lesser extent, this was also true in the case of mutant E363D. When extracellular pH was decreased to 6, channel openings were significantly smaller, as if the channel had only one open state with a low conductance. In mutant E363D the ratio between the open probability of the high and low conductance states was 0.12, 0.43, and 0.64 in the presence of extracellular pH at 6.0, 7.6, and 8.4, respectively. In mutant T364M the open probability of middle and high conductance states at extracellular pH 6.0 was negligible. The concentration of protons in the extracellular medium, however, not only modified the relative probability of the different open states; it also affected the conductance of individual open states with a pK on the order of 4 or 5.

When the intracellular proton concentration was varied in the medium bathing the cytoplasmic side of the membrane, different results were obtained. As shown in Fig. 9, *C* and *D*, changing $[pH]_i$ from 8.4 to 6 significantly increased the open probability for mutants E363D and T364M (five single-channel patches). However, varying $[pH]_i$ did not significantly modify the shape of openings and of amplitude histograms; two open levels in mutant E363D and three

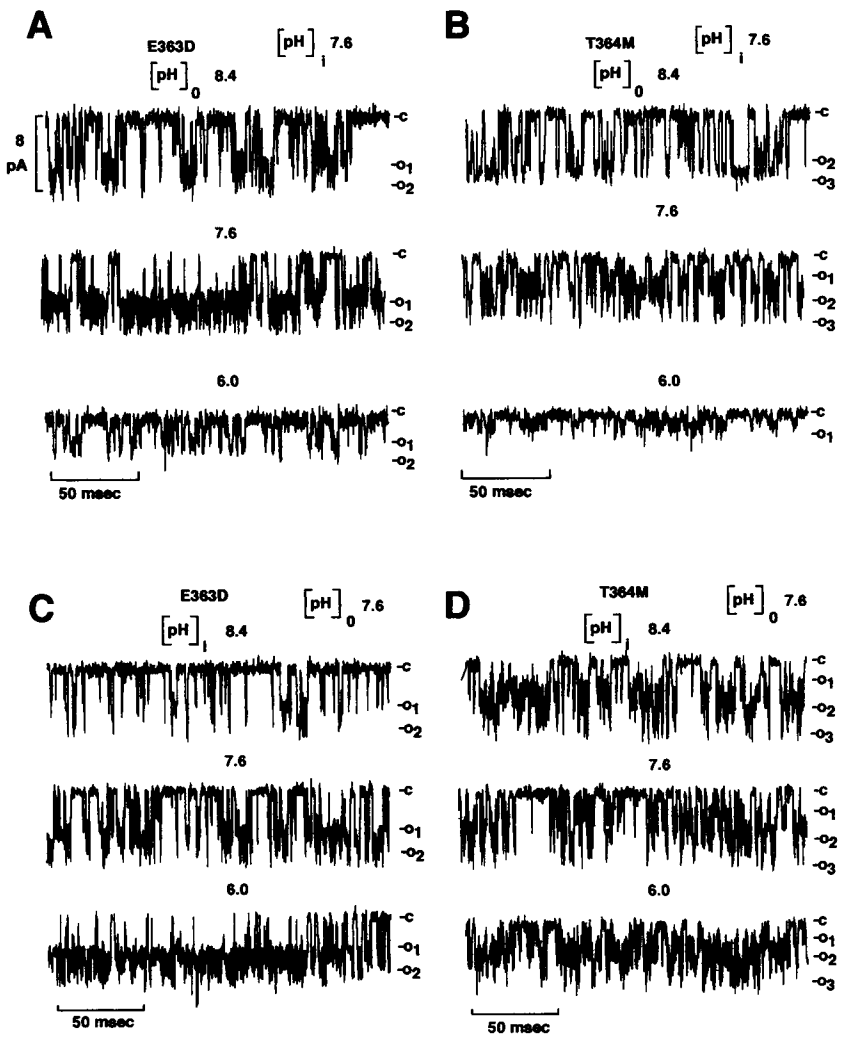

FIGURE 9 Effect of pH on single-channel properties of mutants E363D and T364M at -140 mV. (*A* and *B*) Current recordings from a single channel of mutants E363D (*A*) and T364M (*B*). Upper, middle, and lower rows refer to $[pH]_o$ 8.4, 7.6, and 6, respectively. In *A* and *B* $[pH]_i$ was 7.6. Recordings were from different patches, but were excised from the same oocyte. (*C* and *D*) Current recordings from a single mutant channel E363D and T364M, respectively, in the presence of different $[pH]_i$, but in the presence of $[pH]_o$ in all of the experiments. Channels were activated by 500 μM cGMP added to the medium bathing the intracellular side of the membrane. Current recordings were filtered at 4 kHz and sampled at 20 kHz.

open levels in mutant T364M could be clearly detected in the presence of $[pH]_i$ ranging between 5.5 and 8.4. Increasing the proton concentration slightly decreased the amplitude of channel openings with a pK on the order of 4 or 5. The effect of different pH was analyzed in 8 and 10 single-channel patches of mutants E363D and T364M, respectively. These results indicate a very profound asymmetry of the effect of protons: extracellular protons but not intracellular protons modify the relative probability of the different open states.

When the effect of extracellular protons is analyzed in heteromeric CNG channels, a different result is observed. Fig. 10, *A* and *B*, illustrates current recordings from two different patches containing a single CNG channel obtained by coexpressing the α and β subunits when pH inside the patch pipette was 7.6 and 9.1, respectively. In each panel the upper and lower traces were obtained at +100 and −100 mV, respectively. The current recordings in Fig. 10, *A* and *B*, had the same qualitative flickering behavior. Fig. 10 *C* illustrates a comparison between power spectra of current fluctuations at −100 mV induced by 500 μM cGMP in the presence of extracellular pH 9.1 (*plus signs*) and 7.6 (*diamonds*). The two power spectra have very similar shapes, indicating that the fast flickering observed in CNG channels obtained by coexpressing the α and β subunits is independent of the extracellular proton concentration, similar to what is observed in native CNG channels (Sesti et al., 1994). These results show that the fast flickering in heteromeric channels is not modulated by extracellular protons, whereas the relative probability of different open states in homomeric channels depends on the concentration of extracellular protons.

The gating of CNG channels

As shown in previous figures, openings of CNG channels are not often well resolved, and it is difficult to measure the open times; therefore it is not clear how to characterize their gating in a quantitative way. A possible way is to compute power spectra of current fluctuations induced by cGMP at a given bandwidth. Fig. 11 reproduces power spectra of current fluctuations from different CNG channels at a bandwidth of 10 kHz (see Materials and Methods).

Fig. 11 *A* illustrates power spectra of current fluctuations in the w.t. (*plus signs*) and mutant channels E363D (*diamonds*) and T364M (*triangles*) at −100 mV and in the presence of 500 μM cGMP. These power spectra had broadly the same shape, and about 90% of their energy was concentrated within the band 0–3 kHz. Power spectra of current fluctuations from the w.t. (*plus signs*), mutant E363G (*diamonds*), and the coexpression of the w.t. and mutant E363G (*triangles*) are shown in Fig. 11 *B*. The power spectrum of current fluctuations of mutant E363G had a broader bandwidth, with significant frequency components above 1 kHz, reminiscent of the power spectrum of current fluctuations in the native channel (Sesti et al., 1994). However, the shape of the power spectrum of channels obtained by the coexpression of the w.t. and mutant E363G was more similar to that observed in the w.t. than to that of mutant E363G. These results indicate that the presence of a glycine in the β subunit at the position equivalent to glutamate 363 is not the major origin of the fast flickering observed in type 2 and 3 channels obtained by coexpressing the α and β subunits (see Fig. 11, *D–F*).

The power spectrum of current fluctuations of type 1 channel obtained from the coexpression of the α and β subunit (*diamonds*), shown in Fig. 11 *C*, was only marginally broader than the power spectrum of the w.t. (*plus signs*). In contrast, power spectra of current fluctuations of type 2 and 3 channels were significantly broader than that of the w.t. and extended up to 10 kHz (see Fig. 11 *D*). The frequency cutoff at about 11 kHz, observed in Fig. 11 *D*, could not be distinguished from that expected from the

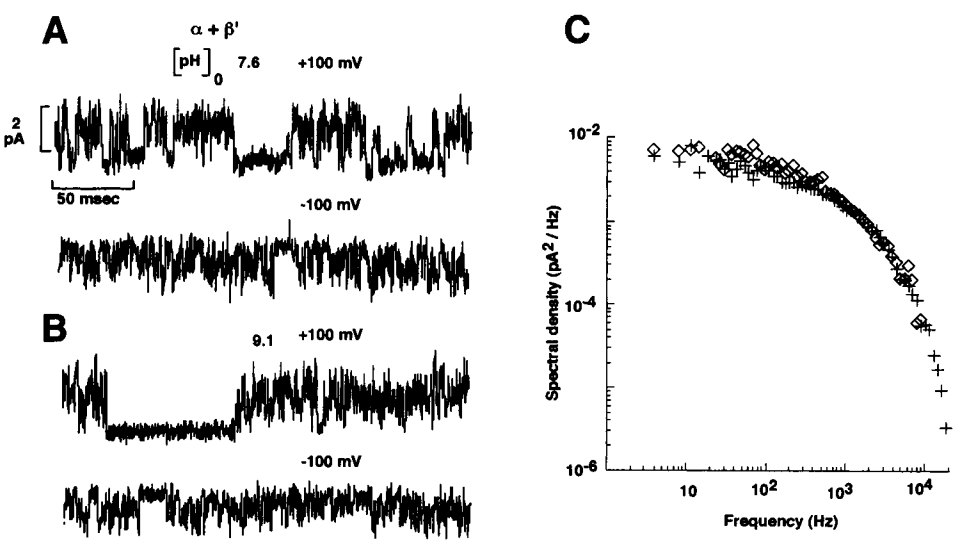

FIGURE 10 Effect of external pH on the coexpression of the α and β subunits. Current recordings from patches containing a single CNG channel obtained from the coexpression of the α and β subunit at $[pH]_o$ 7.6 and 9.1, respectively. In *A* and *B* the upper (*lower trace*) was obtained at +100 (−100) mV. In *A* and *B* recordings were obtained from different patches, but excised from the same oocyte. (*C*) Power spectra of current fluctuations at −100 mV from the experiments shown in *A* (◇) and *B* (+). Current recordings filtered at 20 kHz and sampled at 60 kHz. Power spectra were computed as described by Sesti et al. (1994).

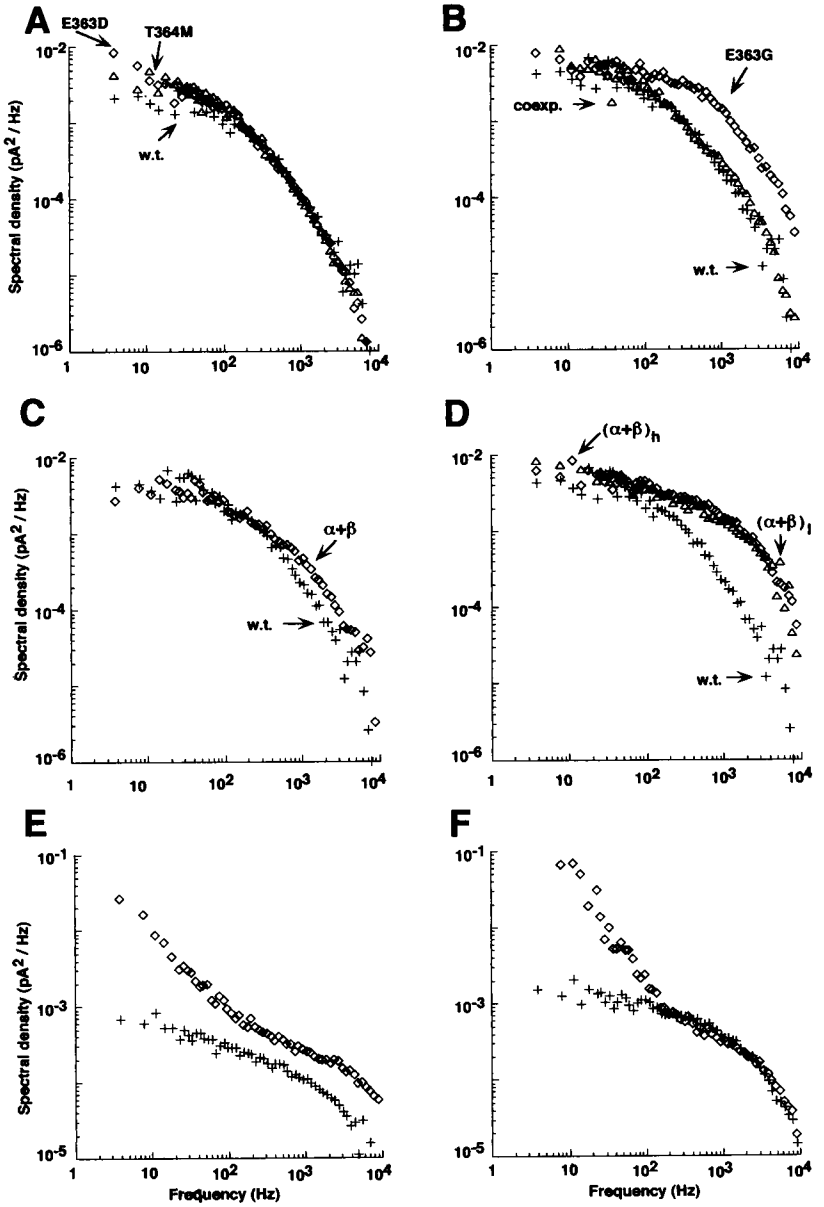

FIGURE 11 Power spectra of the w.t, mutant channels, and coexpressed channels. (*A*) Power spectra of current fluctuations in the presence of 500 μM cGMP at -100 mV from the w.t. (+), mutants E363D (◇) and T364 M (△). (*B*) As in *A*, but for the w.t. (+), mutant E363G (◇), and the coexpression of w.t. and E363G (△). (*C*) As in *A*, but for the w.t (+) and type 1 channel obtained from the coexpression of the α and β subunits (◇). (*D*) As in *A*, but for type 2 (△) and type 3 (◇) of the coexpression of the α and β subunits, indicated by $([\alpha] + [\beta])_l$ and $([\alpha] + [\beta])_h$, respectively. (*E* and *F*) Power spectra at -100 (+) and $+100$ (◇) mV for type 2 and 3 channels obtained from the coexpression of the α and β subunits. Current recordings were filtered at 20 kHz and sampled at 60 kHz. Power spectra were computed as described by Sesti et al. (1994). In *A–D*, power spectra were aligned so as to have a similar low-frequency asymptote.

analog filter used. As a consequence, the real power spectrum of current fluctuations induced by cGMP in type 2 and 3 channels may extend significantly above 10 kHz, as in native CNG channels (Sesti et al., 1994). Fig 11, *E* and *F*, shows power spectra at -100 (*plus signs*) and $+100$ mV (*diamonds*) for type 2 and type 3. The power spectrum in the bandwidth up to 100 Hz has significantly more energy at $+100$ mV than at -100 mV, because of the presence of long closures at positive voltages, lasting several milliseconds, even in the presence of high cGMP concentrations (see Figs. 3 and 4). The shape of the power spectrum above 1 kHz is rather similar at $+100$ and -100 mV, indicating that the fast flickering has similar kinetics properties at negative and positive voltages in the bandwidth up to 10 kHz.

The effect of temperature on single-channel properties

An important physical property of an open pore is the activation energy A_c of the current flowing through it. The activation energy provides an estimate of the enthalpic barrier the ion has to cross during permeation (Sesti et al., 1996). As a consequence, it is important to determine whether the different open states observed in mutant channels have different activation energies. In addition, the analysis of the effect of temperature on the open probability in the presence of a saturating cGMP concentration provides (see Eqs. 3 and 4) an estimate of the Gibbs free energy for the channel gating ΔG_{open}. Therefore we have analyzed the effect of temperature on single-channel properties of the w.t. and mutant channels.

Fig. 12, *A* and *D*, illustrates single-channel recordings at −100 mV at 21°C and 11°C for mutants E363D and T364M, respectively. The corresponding amplitude histograms at 21° (*diamonds*) and at 11°C (*plus signs*) are shown in Fig. 12, *B* and *E*, respectively. It is evident that the open probability increased when the temperature was reduced and that the current flowing through the open states decreased. Fig. 12 *C* shows the dependence of the single-channel current flowing through the high (*plus signs*) and low (*diamonds*) conductance open state on $1/RT$ for mutant E363D. The straight lines through the experimental points indicated an activation energy of 44 and 48 kJ/mol, for the high and low conductance open states. Fig. 12 *F* reproduces a similar dependence for the single-channel current flowing through the middle-conductance open state of mutant T364M. In this case the activation energy was about 44 kJ/mol. The activation energy of the current through an open w.t. channel is about 40 kJ/mol (Sesti et al., 1996). Therefore the activation energy of open channel current in mutants E363D and T364M is slightly higher than in the w.t. channel. These activation energies are higher than the average value of about 25 kJ/mol found in Na^+ channels (Hille, 1992), thus indicating the existence of an enthalpic barrier in CNG channels higher than in Na^+ channels. The relevance of these thermodynamic measurements for ionic permeation has been presented elsewhere (Sesti et al., 1996).

Fig. 13 illustrates the dependence of the open probability on temperature at −100 mV (*diamonds*) in the presence of 1000 μM cGMP for the w.t. (Fig. 13 *A*) and mutant channels E363D (Fig. 13 *B*), T364M (Fig. 13 *C*), and E363G (Fig. 13 *D*). At 21°C, the open probability for the four channels was 0.78 ± 0.06, 0.47 ± 0.14, 0.5 ± 0.12, and 0.007 ± 0.003, respectively. When the temperature was decreased, the open probability remained around 0.8 for the w.t. and significantly increased for the other channels. The gating free energy ΔG_{open} (*plus signs*) was obtained from Eq. 3, and the data shown in Fig. 13 and its dependence on temperature are reported in the same panels of Fig. 13 for the four channels. From these data some thermodynamic quantities characterizing the gating of the four channels can

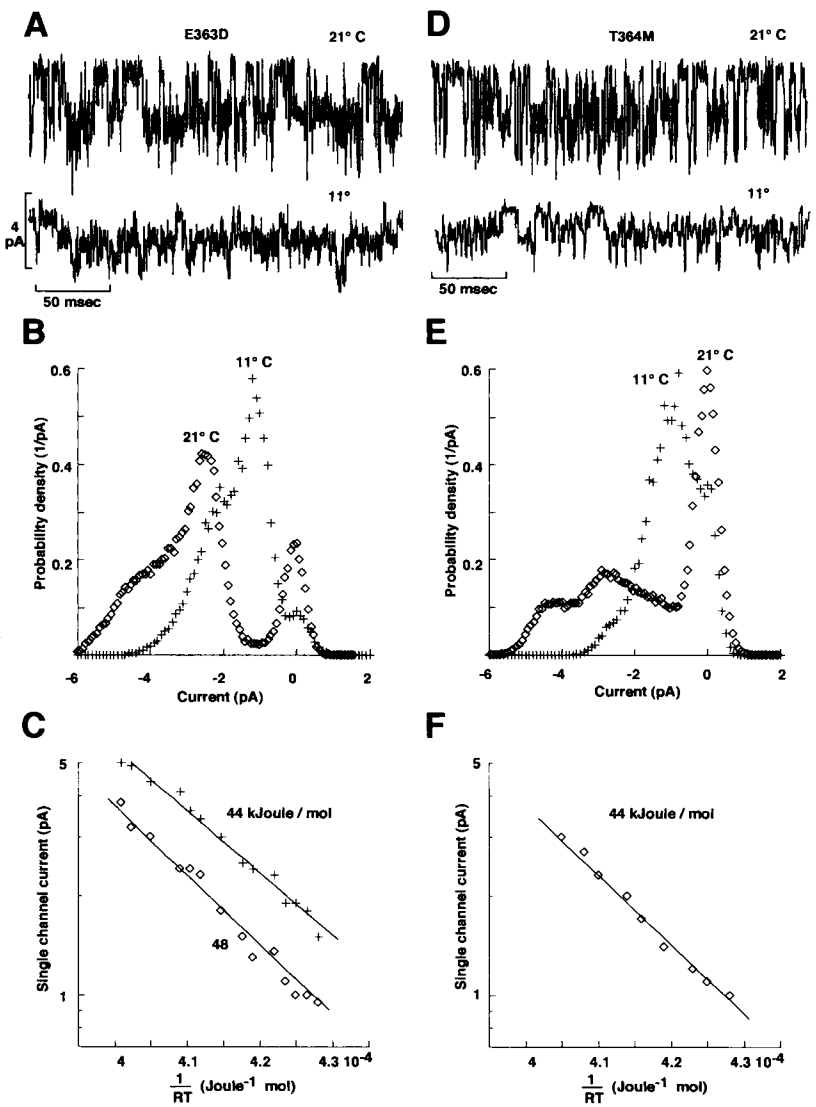

FIGURE 12 The effect of temperature on single-channel properties of mutants E363D and T364M. Channels were activated by 1000 μM cGMP, and the holding voltage was −100 mV. (*A* and *D*) Current recordings at two different temperatures from mutant E363D and T364M, respectively. (*B* and *E*) Amplitude histograms of current openings in *A* and *C*, respectively, at 21°C (◇) and 11°C (+). (*C*) The relation between the single-channel current of mutant E363D of the high (+) and low (◇) conductance state and $1/RT$. The straight lines through the points indicate an activation energy of 44 and 48 kJ/mol for the high and low conductance states, respectively. (*F*) Relation between the single-channel current of the middle conductance state of mutant T364M and $1/RT$. The straight line through the points indicates an activation energy of 44 kJ/mol.

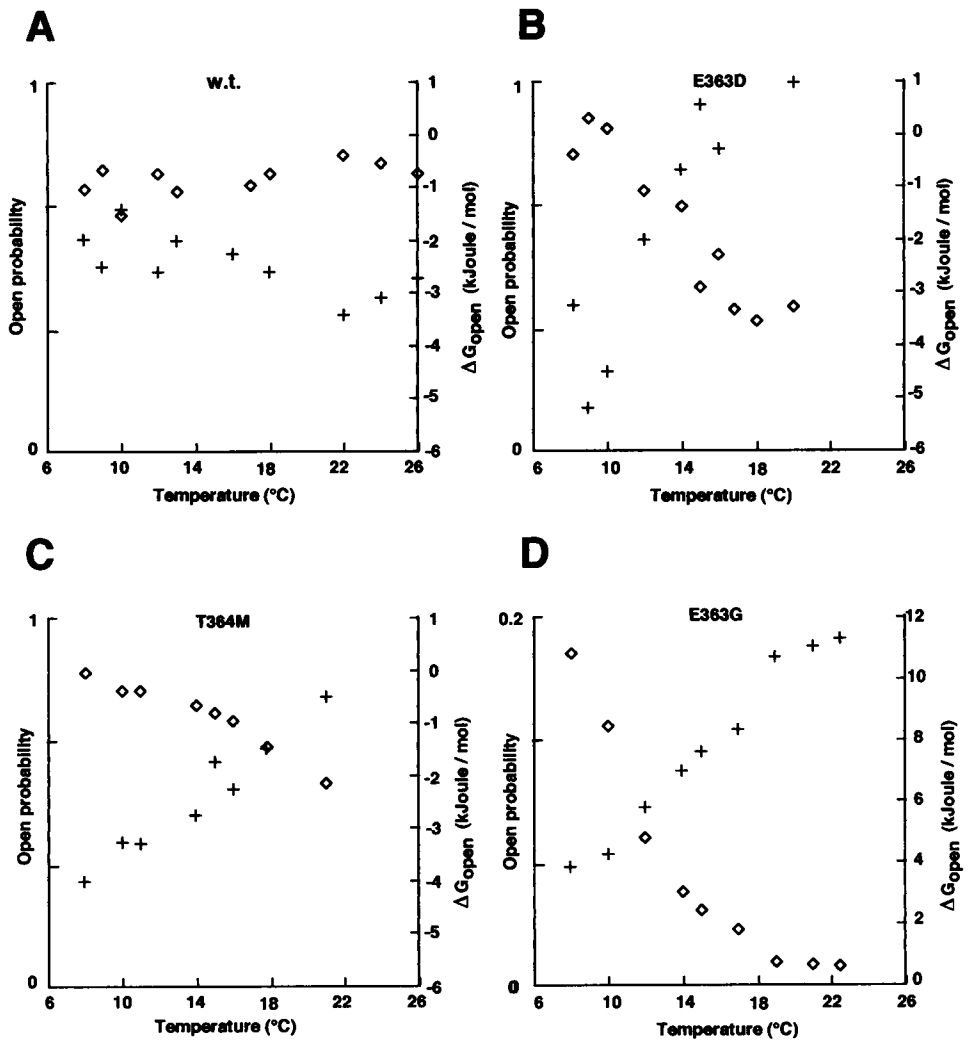

FIGURE 13 The effect of temperature on the open probability in the presence of a saturating cGMP concentration in the w.t. (*A*), mutant E363D (*B*), T364M (*C*), and E363G (*D*). In each panel the open probability (◇) and the opening Gibbs free energy ΔG_{open} (+) are plotted against temperature. The opening Gibbs free energy is defined in Materials and Methods. Channels were activated by 1000 μM cGMP, and the holding voltage was −100 mV.

be obtained. The entropic change ΔS_{open} associated with channel gating can be estimated from Eq. 4. Collected data from at least four patches from the w.t. and mutant channels are shown in Table 1. These values suggest some remarks. At 20°C, the open probability p_o is 0.78 for the w.t., implying a negative value for ΔG_{open} (see Eq. 3). For the two mutants E363D and T364M, p_o is close to 0.5, indicating a value of ΔG_{open} close to 0, whereas for mutant E363G p_o is very small and ΔG_{open} is positive. The entropic contribution ($-T\Delta S_{open}$) is clearly positive for the three mutant channels but very small for the w.t. The enthalpic contribution is negative for the three mutant channels, but small for the w.t. These results indicate that the thermodynamics of the gating in mutant channels is different from that in the w.t.: a large entropic barrier has to be overcome in mutant channels, but not in the w.t.

TABLE 1 The open probability P_o in the presence of 1000 μM cGMP at −100 mV, the Gibbs free energy for the channel gating ΔG_{open} (obtained from Eq. 3), and the enthalpic (ΔH_{open}) and entropic ($-T\Delta S_{open}$) contributions of the channel gating ΔG_{open}

Channel	P_o	ΔG_{open}	ΔH_{open}	$-T\Delta S_{open}$ (kJ/mol)
w.t.	0.78 ± 0.06	−3 ± 0.4	−1 ± 1.9	−2.1 ± 1.5
E363D	0.47 ± 0.14	1 ± 0.8	−79 ± 22.8	80 ± 2.2
T364M	0.5 ± 0.12	0 ± 0.8	−72 ± 18.8	72 ± 18
E363G	0.007 ± 0.003	12 ± 1.5	−120 ± 43.5	132 ± 42

ΔS_{open} was obtained from Eq. 4, and ΔH_{open} was obtained as $\Delta G_{open} + T\Delta S_{open}$. The temperature was 20°.

DISCUSSION

The results presented in this paper suggest that CNG channels usually have multiple open states with different conductances and indicate that the pore region is an essential component of the gating of the channel. Let us review the major issues raised in this paper.

Homomeric CNG channels have multiple open states

The α subunit of CNG channels from vertebrate rods has a single open state or distinct open states with a similar

conductance of about 28 pS (Kaupp et al., 1989; Nizzari et al., 1993). However, when glutamate 363 is mutated to an aspartate or when threonine 364 is mutated to a methionine (see Figs. 6 and 7), or when the α subunit is coexpressed with other polypeptides (see Figs. 2 and 8), distinct open states with a different conductance can be resolved at negative voltages. As shown in Fig. 7, the relative probability of these open states is independent of the cGMP concentration. At -100 mV three open states with a single-channel conductance of about 17, 25, and 43 pS were observed in mutant T364M, whereas only two open states with conductances of 28 pS and 46 pS could be reliably measured in mutant E363D. In contrast, at positive voltages the analysis of amplitude histogram revealed only open states with a conductance of about 28 pS (see Fig. 6).

As in the CNG channel from catfish olfactory sensory neurons, the relative probability of these open states is modulated by the proton concentration in the extracellular medium (Goulding et al., 1992; Root and MacKinnon, 1994), but not significantly in the intracellular medium (see Fig. 9). The single-channel conductance of homomeric CNG channels appears to be sensitive to pH in at least two ways: extracellular protons control the relative probability of the different open states in mutants E363D and T364M with a pK on the order of 7; intracellular protons reduce the single-channel conductance of open state with a pK on the order of 4 or 5. The very weak effect of intracellular protons on the relative probability of the different open states in mutants E363D and T364M indicates the existence of a significant asymmetry very similar to that observed with Ca^{2+}: extracellular Ca^{2+} ions block the CNG channel between 100 and 1000 times more powerfully than intracellular Ca^{2+} (Root and MacKinnon, 1993; Eismann et al., 1994). The asymmetrical action of Ca^{2+} and/or protons cannot be easily explained by interactions within the pore region (Wells and Tanaka, 1996). An alternative explanation is that Ca^{2+} and protons bind to some other domain of the channel.

The w.t. homomeric channel does not exhibit clear open states with a different conductance. However, at very negative voltages the standard deviation of current fluctuations during the open state is about four times that observed when the channel is closed. This observation may suggest that the w.t. homomeric channel also has multiple open states with a similar conductance. These multiple open states may be caused by a different degree of protonation of important residues within the pore of the channel, as suggested by Root and MacKinnon (1994) or by the existence of distinct molecular conformations of the open pore.

The current through open states of mutants E363D and T364M has an activation energy varying between 44 and 48 kJ/mol, slightly higher than that observed in the w.t. channel (Sesti et al., 1996).

Heteromeric CNG channels are heterogeneous

CNG channels obtained by the coexpression of the α and β subunits are heterogeneous and may have different single-channel properties. The present analysis has identified three types of channels: type 1, which has at least two open states with a conductance of about 29 and 44 pS at negative voltages, but a single open state with a conductance of about 40 pS at positive voltages (see Fig. 2); and types 2 and 3, which are characterized by a rapid flickering, very similar to that observed in native CNG channels from vertebrate rods (Sesti et al., 1994; Taylor and Baylor, 1995). At $+100$ mV, type 2 appears to have a lower conductance, whereas type 3 appears to have a higher conductance of at least 45 pS. All three types of channels are blocked by L-*cis*-diltiazem in a voltage-dependent way (see also Chen et al., 1993; Körschen et al., 1995): at $+100$ mV, 50 μM L-*cis*-diltiazem completely blocks channel openings, whereas at -100 mV the same quantity of L-*cis*-diltiazem reduces channel openings from 20 to 50%. The single-channel conductance of the type 1 channel can be reliably estimated, unlike that of types 2 and 3.

In both types 2 and 3 channels, analysis of amplitude histograms at $+100$ mV reveals the existence of a well-resolved peak corresponding to the open state. At negative voltages, even at -200 mV, and at all cGMP concentrations the amplitude histogram is very broad, and no distinct peaks corresponding to the open and closed states can usually be resolved. A very similar behavior has been described in native CNG channels by Taylor and Baylor (1995) and explained by a different gating at positive and negative voltages, with a single channel conductance of 25 pS that is very weakly voltage dependent. However, the data presented in this paper suggest another possible explanation. The analysis of current fluctuations does not indicate any significant difference in the gating of these two channels at -100 and $+100$ mV (see Fig. 11), at least within a bandwidth of up to 10 kHz. The data presented in this paper suggest that CNG channels of types 2 and 3 may have several distinct conductive levels, similar to those observed in type 1. In this view, the fast flickering observed at negative voltages in types 2 and 3 and in native CNG channels is primarily caused by rapid transitions between the closed state and various open states with a different conductance. In contrast, at positive potentials, when there is only one open state or open states with a very similar conductance, the flickering appears to be less prominent.

The existence of different types of channels obtained from the coexpression of the α and β subunits is likely to be caused by a different stoichiometry in which subunits coassemble. However, channels formed by the same number and type of subunits may have different properties because of a different spatial arrangement of subunits within the pore (Liu et al., 1996; Varnum and Zagotta, 1996).

Native CNG channels and heteromeric CNG channels

Single-channel properties obtained by the coexpression of the α and β subunits appear to be very similar to those

observed in native CNG channels. The power spectrum of current fluctuations observed in types 2 and 3 channels (see Fig. 11) extends up to 10 kHz, like the one measured in native channels (Sesti et al., 1994). Current recordings and amplitude histograms of type 2 channel (see Fig. 3) are very similar to those reported by Taylor and Baylor (1995) in some single-channel recordings from outer segments of the tiger salamander.

The present analysis of CNG channels obtained by the coexpression of the α and β subunits indicates the existence of heterogeneous channels, in agreement with a recent report by Karpen and Brown (1996) on native channels. It is not known to what extent types 1 and 3 channels are found in native photoreceptors. However, the heterogeneity of the native CNG channel is also supported by the different single-channel conductance estimates reported in the literature: in an analysis of multiple channel patches, Sesti et al. (1994) obtained an estimate of about 50 pS for the single-channel conductance, similar to that observed in type 3 channel at positive voltages. In their analysis of three single-channel patches, Taylor and Baylor (1995) reported a lower value of 25 pS, consistent with what observed in type 2 channel. However, these estimates of the single-channel conductance in native CNG channels were obtained by assuming that the CNG channels were homogeneous and had only one open conductive state. It is evident from the results reported in this paper that these hypotheses are not verified and that these estimates must be taken with caution. Substates with a different conductance have already been reported in CNG channels (Yau and Baylor, 1989; Taylor and Baylor, 1995). These substates were primarily described at positive voltages, but at these voltages no substates could be reliably observed in the present analysis.

Electrical recordings from patches excised from rod outer segments containing a single native CNG channel are extremely rare, and only three such recordings have been described so far (see Taylor and Baylor, 1995). When patches are excised from rod inner segments (Matthews and Watanabe, 1988; Sesti et al., 1994), single-channel recordings are less difficult to obtain. In contrast, it is rather easy to obtain recordings from single-channel patches from oocytes coinjected with the α and β subunits. In addition, the membrane of oocytes is much more robust than that of native photoreceptors, and stable recordings can be obtained, even in the presence of very large voltages (up to 200 mV), without affecting the membrane integrity. As a consequence, some properties of native CNG channels can be more reliably studied in oocytes coinjected with the α and β subunits.

Coupling of gating and pore region in CNG channels

As shown in Fig. 13, at 21°C, the open probability in the presence of a saturating cGMP concentration (i.e., 1000 μM) is about 0.78, 0.47, 0.5, and 0.007 for the w.t. and mutants E363D, T364M, and E363G, respectively. Given the open probability, we can obtain the change of free energy ΔG_{open} associated with channel opening. In the presence of a saturating cGMP concentration, i.e., when the CNG channel is fully liganded, the transition between the closed and open states does not imply any large change in the Gibbs free energy ΔG_{open} in mutants E363D and T364M, whereas a clear decrease in the w.t. channel and a large increase in mutant E363G are observed. The dependence of the open probability on temperature makes it possible to obtain the enthalpic and entropic contributions of the conformational change leading to channel opening. The data shown in Table 1 indicate that the transition between the fully liganded state and the open state is thermodynamically favorable for the w.t., but not for mutant E363G. These data also show that in mutants E363D, T364M, and E363G the transition to the open state is associated with a decrease in entropy; therefore in these channels a significant entropic barrier has to be crossed during channel opening, i.e., the open state is more ordered than the closed state. These results strongly suggest that the putative pore region is an essential part of the gating structure, but a microscopic interpretation of these thermodynamical measurements is difficult without more direct structural information. Glutamate 363 is thought to be an external binding site (Root and MacKinnon, 1993) located at the narrowest section of the pore of the w.t. channel (Bucossi et al., 1996). As a consequence, the results reported in Fig. 13 indicate that point mutations in the pore region, near the extracellular side, profoundly alter the gating of the channel and change its thermodynamic properties.

These results show that fundamental properties of the gating are controlled by amino acids near the extracellular side of the pore, suggesting that the pore itself is part of the gate. These results also provide additional support to two recent reports, suggesting that the gate of CNG channels is within the pore and that the closing and opening of the CNG channel are associated with conformational changes of the molecular structure within the pore (Sun et al., 1996; Bucossi et al., 1996), further suggesting that the pore region is not rigid, but may exist in different configurations.

The structure of the pore of CNG channels

The existence of distinct open states in homomeric CNG channels, the flickering behavior in heteromeric CNG channels, and the coupling between gating and residues in the pore region suggest, but do not prove, that the inner core of the pore in CNG channels is not a rigid structure. In this view, the flickering behavior observed in heteromeric channels is caused by very rapid transitions between distinct open states with a different conductance. As the flickering behavior is also observed in the presence of an extracellular pH of 9.1 (see Fig. 10), these distinct open states are not caused by a rapid protonation and deprotonation of negatively charged residues, but are likely to be associated with

different molecular configurations of the pore. This behavior of CNG channels is also in agreement with the coupling of the gating and residues in the pore region.

We wish to thank Prof. D. A. Baylor, Prof. B. U. Kaupp, Prof. T. D. Lamb, Dr. A. Menini, and Dr. B. Zagotta for reading the paper and making very useful suggestions. We are grateful to B. U. Kaupp and E. Eismann for providing us with the mRNA for the α and β subunits of the CNG channels from vertebrate rods. Miss L. Giovanelli did the artwork.

This work was supported by EC grants.

REFERENCES

Atkins, P. W. 1978. Physical Chemistry. Oxford University Press.

Baehr, W. B., J. J. Wasmuth, R. L. Harwitz, M. F. Seldim, T. A. Howard, M. R. Althern, A. K. Lee, and S. J. Pittler. 1992. Primary structure and chromosomal localization of human and mouse rod photoreceptor cGMP-gated cation channel. *J. Biol. Chem.* 267:6257–6262.

Baumann, A., S. Frings, M. Godde, R. Seifert, and U. B. Kaupp. 1994. Primary structure and functional expression of a drosophila CNG channel present in eyes and antennae. *EMBO J.* 13:5040–5050.

Bönigk, W., W. Altenhofen, F. Müller, A. Dose, M. Illing, R. S. Molday, and U. B. Kaupp. 1993. Rod and cone photoreceptor cells express distinct genes for cGMP-gated channels. *Neuron.* 10:865–877.

Bradley, J., J. Li, N. Davidson, H. Lester, and K. Zinn. 1994. Heteromeric olfactory cyclic nucleotide gated channels; a subunit that confers increased sensitivity to cAMP. *Proc. Natl. Acad. Sci. USA.* 91:8890–8894.

Bucossi, G., E. Eismann, F. Sesti, M. Nizzari, M. Seri, U. B. Kaupp, and V. Torre. 1996. Time dependent current decline in cyclic GMP gated channels caused by point mutations in the pore region. *J. Physiol. (Lond.).* 493.2:409–418.

Chen, T. Y., Y. W. Peng, R. S. Dhallan, B. Ahamed, R. R. Reed, and K. W. Yau. 1993. A new subunit of the cyclic nucleotide-gated cation channel in retinal rods. *Nature.* 362:764–767.

Dhallan, R. S., J. P. Macke, R. L. Eddy, T. B. Shows, R. S. Reed, K. W. Yau, and J. Matthews. 1992. Human rod photoreceptors cGMP-gated channel: amino acid sequence, gene structure and functional expression. *J. Neurosci.* 12:3248–3256.

Dhallan, R. S., K. W. Yau, K. A. Schrader, and R. R. Reed. 1990. Primary structure and functional expression of a cyclic nucleotide-activated channel from olfactory neurons. *Nature.* 347:184–187.

Eismann, E., F. Müller, S. Heinemann, and B. Kaupp. 1994. A single negative charge within the pore region of a cGMP-gated channel controls rectification, Ca^{2+} blockage, and ionic selectivity. *Proc. Natl. Acad. Sci. USA.* 91:1109–1113.

Frings, S., R. Seifert, M. Godde, and U. B. Kaupp. 1995. Profoundly different calcium permeation and blockage determine the specific function of distinct cyclic nucleotide-gated channels. *Neuron.* 169–179.

Gavazzo, P., C. Picco, L. Maxia, and A. Menini. 1996. Properties of native and cloned cyclic nucleotide gated channels from bovine. *In* Neurobiology. Plenum Press, New York.

Gordon, S. E., and W. N. Zagotta. 1995. Localization of regions affecting an allosteric transition in cyclic nucleotide-activated channels. *Neuron.* 14:857–864.

Goulding, E. H., J. Ngai, R. H. Kramer, S. Colicos, R. Axel, S. A. Siegelbaum, and A. Chess. 1992. Molecular cloning and single channel properties of the cyclic nucleotide-gated channel from catfish olfactory neurons. *Neuron.* 8:45–58.

Goulding, E. H., G. R. Tibbs, and S. A. Siegelbaum. 1994. Molecular mechanism of cyclic nucleotide-gated channel activation. *Nature.* 372:369–374.

Hamill, O. P., A. Marty, E. Neher, B. Sakmann, and F. J. Sigworth. 1981. Improved patch-clamp techniques for high resolution current recording from cells and cell-free membrane patches. *Pflugers Arch.* 391:85–100.

Hille, B. 1992. Ionic Channels of Excitable Membranes. Sinauer Associates, Sunderland, MA.

Karpen, J. W., and R. L. Brown. 1996. Covalent activation of retinal rod cGMP-gated channels reveals a functional heterogeneity in the ligand binding sites. *J. Gen. Physiol.* 107:169–181.

Kaupp, U. B. 1995. Family of cyclic nucleotide-gated channels. *Curr. Opin. Neurobiol.* 5:434–442.

Kaupp, U. B., T. Niidome, T. Tanabe, S. Terada, W. Bonigk, W. Stuehmer, N. J. Cook, K. Kangawa, H. Matsuo, T. Hirose, T. Miyata, and S. Numa. 1989. Primary structure and functional expression from complementary DNA of the rod photoreceptor cyclic GMP-gated channel. *Nature.* 342:762- 766.

Körschen, H., M. Illing, R. Seifert, F. Sesti, A. Williams, S. Gotzes, S. Colville, F. Miller, A. Dose, M. Godde, L. Molday, U. B. Kaupp, and R. S. Molday. 1995. A 240 K protein with a bipartite structure represents the complete β-subunit of the cyclic nucleotide-gated channel from rod photoreceptor. *Neuron.* 15:627–636.

Liu, D. T., G. R. Tibbs, and S. A. Siegelbaum. 1996. Subunit stoichiometry of cyclic nucleotide gated channels and effects on subunit order or channel function. *Neuron.* 16:983–990.

Ludwig, J., T. Marglit, E. Eismann, D. Lancet, and U. B. Kaupp. 1990. Primary structure of a cAMP-gated channel from bovine olfactory epithelium. *FEBS Lett.* 270:24–29.

Matthews, G., and S-I. Watanabe. 1988. Activation of single ion channels from toad retinal rod inner segments by cyclic GMP. *J. Physiol. (Lond.).* 403:389–405.

Nizzari, M., F. Sesti, M. T. Giraudo, C. Virginio, A. Cattaneo, and V. Torre. 1993. Single channel properties of a cloned channel activated by cGMP. *Proc. R. Soc. Lond.* 254:69–74.

Park, C. S., and R. MacKinnon. 1995. Divalent cation selectivity of an ion binding site in the pore of a cyclic nucleotide-gated channel. *Biochemistry.* 34:13328–13333.

Root, M. J., and R. MacKinnon. 1993. Identification of an external divalent binding site in the pore of a cGMP-activated channel. *Neuron.* 11:459–466.

Root, M. J., and R. MacKinnon. 1994. Two identical non interacting sites in an ion channel revealed by proton transfer. *Science.* 265:1852–1856.

Sesti, F., E. Eismann, B. U. Kaupp, M. Nizzari, and V. Torre. 1995. The multi-ion nature of the cGMP-gated channel from vertebrate rods. *J. Physiol. (Lond.).* 487-1:17–36.

Sesti, F., M. Nizzari, and V. Torre. 1996. The effect of changing the temperature on the ionic permeation through the cyclic GMP-gated channel from vertebrate photoreceptors. *Biophys. J.* 70:2616–2639.

Sesti, F., M. Straforini, T. D. Lamb, and V. Torre. 1994. Properties of single channels activated by cyclic GMPin retinal rods of the tiger salamander. *J. Physiol. (Lond.).* 474-2:203–222.

Stern, J. H., U. B. Kaupp, and P. R. McLeish. 1986. Control of the light-regulated current in photoreceptors by cyclic GMP, calcium and l-*cis*-diltiazem. *Proc. Natl. Acad. Sci. USA* 83:1163–1167.

Sun, Z-P., M. H. Akabas, E. H. Goulding, A. Karlin, and S. Siegelbaum. 1996. Exposure of residues in the cyclic nucleotide gated channel pore: P region structure and function in gating. *Neuron.* 16:141–149.

Taylor, W. R., and D. A. Baylor. 1995. Conductance and kinetics of single cGMP-activated channels in salamander rod outer segments. *J. Physiol. (Lond.).* 483:567–582.

Varnum, M. D., K. D. Black, and W. N. Zagotta. 1995. Molecular mechanisms for ligand discrimination of cyclic nucleotide gated channels. *Neuron.* 15:619–625.

Varnum, M. D., and W. N. Zagotta. 1996. Subunit interactions in the activation of cyclic nucleotide gated ion channels. *Biophys. J.* 70:2667–2679.

Wells, G. B., and J. C. Tanaka. 1997. Ion selectivity predictions from a two site permeation model for the cyclic nucleotide-gated channel of retinal rod cells. *Biophys. J.* (in press).

Weyand, I., M. Godde, S. Frings, J. Weiner, F. Müller, W. Altenhofen, H. Hatt, and U. B. Kaupp. 1994. Cloning and functional expression of a cyclic nucleotide gated channel from mammalian sperm. *Nature.* 368:859–863.

Yau, K. W., and D. A. Baylor. 1989. Cyclic GMP-activated conductance of retinal photoreceptor cells. *Annu. Rev. Neurosci.* 12:289–327.